RSC Advances

PAPER

View Article Online
View Journal | View Issue

Cite this: *RSC Adv.*, 2024, **14**, 4778

Streptomyces monashensis MSK03-mediated synthesis of gold nanoparticles: characterization and antibacterial activity

Supavadee Kerdtoob,[a] Panjamaphon Chanthasena,[b] A'liyatur Rosyidah,[c] Wanwisa Limphirat,[d] Watsana Penkhrue,[a] Phongsakorn Ganta,[a] Wissarut Srisakvarangkool,[a] Montri Yasawong[ef] and Nawarat Nantapong *[a]

Nanotechnology is a cutting-edge field with diverse applications, particularly in the utilization of gold nanoparticles (AuNPs) due to their stability and biocompatibility. AuNPs serve as pivotal components in medical applications, with a specific emphasis on their significant antibacterial efficacy. This study focuses on synthesizing AuNPs using the cell-free supernatant of *Streptomyces monashensis* MSK03, isolated from terrestrial soil in Thailand. The biosynthesis process involved utilizing the cell-free supernatant of *S. monashensis* MSK03 and hydrogen tetrachloroauric acid ($HAuCl_4$) under controlled conditions of 37 °C and 200 rpm agitation. Characterization studies revealed spherical AuNPs with sizes ranging from 7.1 to 40.0 nm (average size: 23.2 ± 10.7 nm), as confirmed by TEM. UV-Vis spectroscopy indicated a localized surface plasmon resonance (LSPR) band at 545 nm, while XRD analysis confirmed a crystalline structure with characteristics of cubic lattice surfaces. The capping molecules on the surface of AuNPs carry a negative charge, indicated by a Zeta potential of −26.35 mV, and FTIR analysis identified functional groups involved in reduction and stabilization. XANES spectra further confirmed the successful reduction of Au^{3+} to Au^0. Moreover, the synthesized AuNPs demonstrated antibacterial activity against drug-resistant strains of *Pseudomonas aeruginosa* and *Acinetobacter baumannii*. Interestingly, the AuNPs showed non-toxicity to Vero cell lines. These significant antibacterial properties of the produced nanoparticles mean they hold great promise as new antimicrobial treatments for tackling the increasing issue of antibiotic resistance.

Received 5th November 2023
Accepted 28th January 2024

DOI: 10.1039/d3ra07555a

rsc.li/rsc-advances

Introduction

In recent years, there has been a surge of interest in nanotechnology for the production of metal nanoparticles (NPs).[1,2] This field involves manipulating nanosized materials (1–100 nm) to generate novel features such as chemical, biological, electrical, and catalytic qualities that bulk materials cannot attain.[3,4] Metal nanoparticles find wide-ranging applications in medicine and materials engineering.[2,3,5–8] For instance, gold nanoparticles synthesized using a combination of five cow-derived products (urine, dung, milk, curd, ghee) showed antimicrobial activity against human pathogens, *Klebsiella pneumoniae* and *Bacillus subtilis*. Copper iodide nanoparticles were used for monitoring of dopamine, aiding in the early diagnosis of neurodegenerative disorders.[9] Additionally, the determination of vitamin B12 (VB12) was achieved by developing an electrochemical sensor prepared through the electrophoretic deposition of tin dioxide nanoparticles.[6] Furthermore, titanium carbide–MXene nanoparticles were produced using plastic and applied in a self-charging device.[7]

Among NPs, gold nanoparticles (AuNPs) have been studied extensively by many researchers due to their unique properties, such as antimicrobial activity, low toxicity, ease of production, and precision targeting.[2,10,11] Recently, there has been a lot of research focused on antibacterial properties of AuNPs making them a promising candidate for antibiotic supplementation. The antibacterial activity of AuNPs is determined by several factors, including size, dose, and the type of bacteria.[2,3] Previous studies by Shamaila and colleagues demonstrated that chemically synthesized AuNPs exhibit antibacterial action against *Staphylococcus aureus*, *Escherichia coli*, *K. pneumoniae*, and *B. subtilis*, with the activity being size and dose-dependent.[2]

[a]*School of Preclinical Sciences, Institute of Science, Suranaree University of Technology, Nakhon Ratchasima 30000, Thailand. E-mail: nawarat@sut.ac.th*

[b]*Department of Medical Technology, Faculty of Allied Health Sciences, Nakhonratchasima College, Nakhon Ratchasima 30000, Thailand*

[c]*Research Center for Vaccine and Drug, National Research and Innovation Agency (BRIN), Bogor, West Java, Indonesia*

[d]*Synchrotron Light Research Institute, 111 University Avenue, Nakhon Ratchasima, Thailand*

[e]*Programme on Environmental Toxicology, Chulabhorn Graduate Institute, Bangkok 10210, Thailand*

[f]*Center of Excellence on Environmental Health and Toxicology (EHT), OPS, MHESI, Bangkok 10400, Thailand*

Furthermore, different types of bacteria showed distinct responses to AuNPs. For example, the antibacterial activity of biologically synthesized PG-AuNPs by panchagavya (PG) was found to be strong against Gram-negative bacteria and moderate against Gram-positive bacteria.[3]

The synthesis of AuNPs can be achieved through chemical, physical, and biological methods.[1] However, chemical and physical approaches, which often involve the use of toxic agents, raise concerns for both the environment and human health. In contrast, biological synthesis is considered a safe, non-toxic, and environmentally friendly alternative.[1,3,12,13] This approach entails the utilization of bacteria, fungi, plants, and other natural raw materials for the synthesis of nanoparticles.[3] Microorganisms, especially *Streptomyces* species, are effective in producing AuNPs due to their ability to grow in a low-cost medium and facilitate controlled reduction of metal ions.[14] *Streptomycetes*, Gram-positive filamentous bacteria that serve as a valuable source of antibiotics, have proven the potential to synthesize AuNPs.[15] Previous reports highlight various *Streptomyces* species, such as *Streptomyces cyaneus* Alex-SK121, *Streptomyces* sp. NH21, *Streptomyces hygroscopicus* BDUS49, *Streptomyces griseus* M8, *Streptomyces misionensis* PYA9, *Streptomyces* sp. U30, and *Streptomyces viridogens* HM10, in the synthesis of AuNPs with antimicrobial activity against various bacteria.[16–22]

In this study, we synthesized AuNPs using the cell-free supernatant of *Streptomyces monashensis* MSK03, isolated from terrestrial soil in Thailand. The biosynthesis of AuNPs was characterized using various techniques, including UV–visible spectroscopy, X-ray diffraction (XRD) spectroscopy, energy-dispersive X-ray (EDX) spectroscopy, transmission electron microscopy (TEM), Fourier transform infrared (FTIR) spectroscopy, and X-ray absorption near edge structure (XANES) spectroscopy. Additionally, we explored the antibacterial potential of these nanoparticles against clinical drug-resistant pathogens and assessed their cytotoxicity profiles. To our knowledge, this is the first report on the utilization of *S. monashensis* for synthesizing AuNPs. Our findings significantly contribute to understanding the potential of *Streptomyces* species in the field of nanoparticle biosynthesis, paving the way for future research and applications.

Experimental

Microorganisms

Streptomyces sp. MSK03 was isolated from terrestrial soil at Sakaerat Environmental Research Station (SERS), Nakhon Ratchasima, Thailand. To assess the antimicrobial activity, drug-resistant strains of *Pseudomonas aeruginosa* and *Acinetobacter baumannii* were used. These pathogenic bacteria were obtained from clinical samples at Suranaree University of Technology Hospital (SUTH), Thailand.

Isolation of *Streptomyces* sp. MSK03

Soil samples were randomly collected randomly from the upper surface of the soil at a depth of 10–15 cm using a sterile technique. A total of 1 g of soil was suspended in 99 mL of sterile water and incubated at room temperature with shaking at 200 rpm for 30 minutes. After incubation, the soil suspension was allowed to settle, and then it was subjected to 10-fold serial dilution up to 10^{-6}. The *Streptomyces* strain was isolated using the actinomycete isolation agar (AIA, Himedia, India) medium through a serial dilution procedure. The agar plates were incubated at 37 °C for a duration of 7 days or until the colonies appeared. The streptomycetes colonies were further purified on International *Streptomyces* Project 2 (ISP2) agar medium (4 g L^{-1} of yeast extract, 10 g L^{-1} of malt extract, 4 g L^{-1} of glucose, 15 g L^{-1} of agar, and pH 7.2).

Identification of *Streptomyces* sp. MSK03

For molecular identification of *Streptomyces* sp. strain MSK03, genomic DNA was extracted using the modified method for fungal DNA extraction.[23] The 16S ribosomal RNA (rRNA) gene was amplified using polymerase chain reaction (PCR) with universal 16S rRNA primers, 27F 5′ AGAGTTTGATCCTGGCTCAG 3′ and 1525R 5′ AAGGAGGTGWTCCARCC 3′.[24] The PCR product was then purified using the Gel/PCR Purification Mini Kit (Favorgen™, Taiwan), and the purified PCR products were sent for sequencing at Macrogen, Korea. The sequence of the 16S rRNA gene was compared to the EzBioCloud 16S rRNA database (**http://www.ezbiocloud.net**) for identification purposes.

Preparation of cell-free supernatant

Streptomyces sp. MSK03 was cultured in a 500 mL Erlenmeyer flask with 100 mL of Starch Casein Broth (SCB) (10 g L^{-1} of soluble starch, 0.3 g L^{-1} of casein, 2 g L^{-1} of KNO_3, 2 g L^{-1} of NaCl, 2 g L^{-1} of K_2HPO_4, 0.05 g L^{-1} of $MgSO_4$, 0.02 g L^{-1} of $CaCO_3$, 0.01 g L^{-1} of $FeSO_4$, and pH 7.2) and incubated at 37 °C under shaking conditions at 200 rpm for 5 days. After the incubation period, the culture was centrifuged at 4 °C and 8000 rpm for 5 minutes. The resulting cell-free supernatant was carefully collected and utilized for the biosynthesis of AuNPs.

Biosynthesis of AuNPs

Biosynthesis of AuNPs was carried out by following the methods outlined by Khadivi *et al.*,[12] Soltani *et al.*,[25] and Balagurunathan *et al.*[22] with minor modification. In brief, 1 mM Hydrogen tetra chloroauric acid ($HAuCl_4 \cdot 3H_2O$; Sigma-Aldrich, USA.) was combined with the cell-free supernatant of *Streptomyces* sp. MSK03 at a 1 : 1 volume-to-volume ratio. The reaction mixture underwent an incubation period at 37 °C with continuous shaking at 200 rpm for 72 hours, and the pH was adjusted to 7. As a control experiment, the cell-free supernatant and $HAuCl_4$ solution was used. After the incubation period, the synthesis of AuNPs was visually monitored as the mixture transitioned from a pale yellow hue to a pale pink or purple color. This distinctive color change served as a visible marker for the successful reduction of Au^{3+} to Au^0, a key milestone in the biosynthesis process. The entire mixture was centrifuged at 4 °C, 8000 rpm for 5 minutes, and the AuNPs were washed with sterile DI water, then collected for further studies.

Characterization of MSK03-AuNPs

UV-vis spectroscopy analysis. The biosynthesized AuNPs were subjected to characterization using a UV-visible spectrophotometer (Thermo Scientific Multiscan GO, Finland). The absorbance of colloidal AuNPs was measured, and the absorption spectra were recorded within the wavelength range of approximately 300–800 nm.[12,16,18,22,25–28] This analysis allowed for the evaluation of the optical properties of the AuNPs and the determination of their absorbance characteristics.

X-ray diffraction (XRD) analysis. The crystallinity and the X-ray diffractive pattern of the MSK03-AuNPs were determined by XRD analysis using an X-ray diffractometer (D8 Advance, Bruker, Germany) employing nickel-filtered Cu Kα radiation (λ = 1.5406 E; 40 kV, 30 mA) in the 2θ range of 20–80° at 25 °C, with a scan speed of 10° min^{-1}. The diffraction peaks of the AuNPs were compared to a standard XRD pattern for the structure of AuNPs, which is referenced as Joint Committee on Powder Diffraction Standards (JCPDS) no. 04-0784. This standard is part of a database of XRD patterns maintained by the International Center for Diffraction Data. By comparing the obtained diffraction peaks with this reference, the crystalline structure and identity of the synthesized AuNPs were determined.[12,16,18,22,25–28]

Zeta potential and hydrodynamic size distribution analysis. Zeta potential measurement and hydrodynamic particle size distribution analysis of the MSK03-AuNPs were conducted using a Zeta-sizer instrument (Malvern Instrument Ltd, USA). The zeta potential analyzer was utilized to measure the zeta potential, indicating the surface charge of the AuNPs.[27,28] On the other hand, the dynamic light scattering (DLS) technique was employed to measure the average particle size distribution of the biosynthesized AuNPs.[16,28,29]

Transmittance electron microscopy (TEM) and energy dispersive X-ray fluorescence (EDX) spectrometry analysis. TEM (Talos F200X, Thermo Scientific, Netherlands) was utilized to examine the size and morphology of the biosynthesized AuNPs. Additionally, Transmission Electron Microscopy (TEM) was employed to investigate Selected Area Electron Diffraction (SAED).[6,17,30] Moreover, the elemental composition and chemical characterization of the synthesized AuNPs were determined through EDX spectroscopy analysis using an X-ray Fluorescence Energy Dispersive Spectrometer (Model XGT-5200).[18,25,28,31,32]

Fourier transform infrared (FTIR) spectroscopy analysis. FTIR spectroscopy was employed to identify potential biological molecules involved in the reduction of Au^{3+} to Au^{0} during the biosynthesis of AuNPs.[16,28,33] The FTIR spectrophotometer used for this analysis was the FT-IR microscope (Tensor 27, Bruker, Germany). The spectra were scanned in the range of 400–4000 cm^{-1}, allowing for the detection of functional groups of organic molecules that may be attached to the surface of AuNPs. Additionally, other surface chemical residues were also identified through FTIR analysis. The obtained spectral data were compared with an online database to aid in the characterization and identification of the chemical compounds present in the biosynthesized AuNPs.

X-ray absorption near-edge spectroscopy (XANES) analysis. XANES analysis was conducted to investigate the local geometry and structure of gold in the synthesized MSK03-AuNPs.[34,35] The photon energy was calibrated using the L3 edge of Au (foil) at 11 919 eV. The obtained XANES data was averaged and normalized using the Demeter package, version 8.9.26.32. This XANES analysis was carried out at the XANES beamline (beamline 8) at the Synchrotron Light Research Institute (SLRI), Thailand.

Determination of the antimicrobial activity of AuNPs

The antimicrobial activity of MSK03-AuNPs against drug-resistant pathogens *P. aeruginosa* and *A. baumannii* was assessed using the agar well diffusion method. The Mueller–Hinton agar (Himedia™, India) was inoculated with mid-log phase (5×10^5 CFU mL^{-1}) test pathogens using the spread plate technique. Subsequently, a 6 mm diameter hole was aseptically punched in the agar using a sterile cork borer. One hundred microliters of the MSK03-AuNPs (56.55 μg) were then added into the well and allowed to diffuse into the agar at room temperature for 1 hour. The culture broth of MSK03 and $HAuCl_4$ were used as control substances. Following this, all plates were incubated at 37 °C for 24 hours. The formation of a clear zone around the well was observed and measured to determine the antimicrobial activity of MSK03-AuNPs against the drug-resistant pathogens.

Cytotoxicity assay

The MTT assay was performed to analyze the inhibitory concentration (IC_{50}) of synthesized AuNPs.[36–38] The Vero cell line (kidney tissue of an African green monkey) was cultured in Dulbecco's Modified Eagle Medium (DMEM) supplemented with 10% Fetal Bovine Serum (FBS). A total of 10^4 cells per well were seeded in 96-well plates and incubated at 37 °C with 5% CO_2 for 24 hours. After 24 hours, the cells were treated with different concentrations of MSK03-AuNPs (ranging from 32 to 512 μg mL^{-1}) in serum-free media and incubated for an additional 24 hours. Subsequently, the cells were treated with MTT (0.5 mg mL^{-1}) and incubated for 4 hours to allow the formation of formazan crystals. The formed formazan crystals were solubilized by removing the MTT solution and adding 100 μL of 100% DMSO : 10% SDS (9 : 1) to each well. The absorbance of the purple-blue formazan dye was then measured at 570 nm using a spectrophotometer. The percentage cytotoxicity of each concentration was calculated and utilized for IC_{50} determination using the GraphPad Prism 5.0 program.

Results and discussion

Isolation and identification of *Streptomyces* sp. MSK03

Streptomyces is the genus of the actinomycetales order with more than 500 members, including those industrially significant for their unrivaled ability to produce a wide range of bioactive secondary metabolites with interesting biological activities.[15] The present study attempted to eco-friendly synthesizes AuNPs using the soil bacterium *Streptomyces* sp. MSK03 and investigated their biological properties, particularly

antibacterial and cytotoxic effects. The strain MSK03 was isolated from forest soil at SERS, Nakhon Ratchasima province, Thailand. The identification of *Streptomyces* sp. MSK03 was based on its physiological and morphological properties, as depicted in Fig. 1. The strain exhibited leathery growth with white aerial mycelium and dark yellow substrate mycelium on ISP2 medium, and its colony released light yellow soluble pigments visible as exudates after incubation at 37 °C for 10 days.

Molecular techniques based on 16S rRNA gene sequences were employed to identify the species level of bacterial strain.[39] The 16S rRNA gene sequence of strain MSK03 was amplified using 27F and 1525R primers.[24] The 16S rRNA gene sequence of MSK03 was submitted to GenBank with the accession number ON159854. The 16S rRNA of MSK03 showed a high similarity of 99.79% to *Streptomyces monashensis* MUSC $1J^T$ (KP998432). Organisms are typically identified at the species level when their 16S rRNA gene sequences exhibit more than 99% identity.[39] Thus, we propose that strain MSK03 belongs to the *S. monashensis* species, which, to our knowledge, has not been previously employed in metal nanoparticle synthesis.

Biosynthesis of MSK03-AuNPs

The use of streptomycetes in gold nanoparticle (AuNP) biosynthesis offers a versatile and advantageous approach.[14,15,40] With inherent biocompatibility and low toxicity, streptomycetes are well-suited for biomedical applications.[14,15] Their enzymatic activity serves as eco-friendly reducing and stabilizing agents, while their metal-tolerant nature facilitates efficient nanoparticle reduction.[14,41] The controlled synthesis allows for fine-tuning of AuNPs size and shape.[42–44] Streptomycetes' abundance and diversity in natural environments provide a rich resource for strain optimization, ensuring economic viability and environmental friendliness in large-scale production.[14,15] Furthermore, the potential for nanoparticle functionalization and antibacterial properties further underscores the diverse benefits of employing streptomycetes in AuNP biosynthesis.[42,43,45] In this study, AuNPs were synthesized using the extracellular cell-free supernatant of *S. monashensis* MSK03, which acted as reducing and stabilizing agents. The synthesis process involved mixing the cell-free supernatant of MSK03 with 1 mM $HAuCl_4$ in a 1 : 1 ratio, followed by incubation at 37 °C for 72 hours. The initial light yellow mixture changed noticeably during incubation into a purple color, demonstrating the formation of surface plasmon resonance (SPR), characteristic of AuNPs (Fig. 2). The color of the solution changed from light yellow to purple upon the formation of AuNPs, indicating that Au^{3+} was reduced to Au^0.[22,29,46–50] Thus, *S. monashensis* MSK03 demonstrated successful biosynthesis of AuNPs, a capability not shared by all *Streptomyces* strains. This study leads the recognition of *S. monashensis* as a novel candidate for the eco-friendly synthesis of AuNPs, marking an unexplored avenue in nanoparticle biosynthesis research.

Characterization of gold nanoparticles

To confirm the formation of AuNPs, UV-Vis spectrophotometry techniques were employed to determine the position of the localized surface plasmon resonance (LSPR) bands of the synthesized AuNPs.[22,29,48,51] The LSPR band of MSK03-AuNPs exhibited a wavelength of maximum absorbance at 545 nm, falling within the absorption range typically observed for spherical AuNPs (500–580 nm).[43,52,53] In contrast, no absorption spectrum corresponding to AuNPs was observed in the cell-free supernatants or $HAuCl_4$ solutions, as depicted in Fig. 3. This confirmed that the characteristic absorption peak at 545 nm was indeed due to the presence of the synthesized AuNPs, confirming the existence of spherical AuNPs produced by *S. monashensis* MSK03.

In this study, multiple analyses were performed to demonstrate the formation of AuNPs, including EDXRF, XRD, and XANES.[25,33,54] The elemental mapping obtained from TEM-EDXRF and XRD techniques confirmed the presence of Au elements in the sample. The EDXRF spectra indicated strong optical absorption peaks corresponding to metallic Au at 2.2, 9.7, and 11.5 keV, with the Au element detected at 8.08% in the MSK03-AuNPs (Fig. 4). The crystal structure of MSK03-AuNPs was elucidated through XRD analysis, as shown in Fig. 5. The XRD pattern exhibited four distinct diffraction peaks at 2θ values of 38.3°, 44.5°, 64.9°, and 77.8°, corresponding to the (111), (200), (220), and (311) crystallographic planes, respectively, of the face-centered cubic (fcc) structure of metallic gold. This unequivocally confirmed that the crystal structure of MSK03-AuNPs exhibited the characteristic features of a cubic lattice surface.

Fig. 1 Colony morphology of soil-isolated *S. monashensis* MSK03 on ISP2 agar after 10 days of incubation.

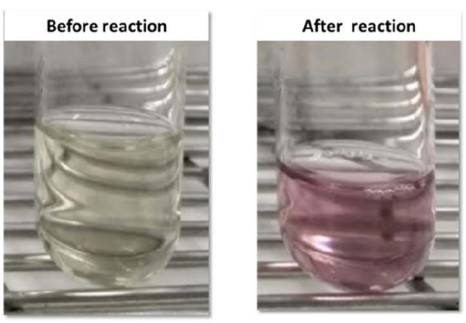

Fig. 2 Visual observation of the color change of biosynthesized AuNPs by *S. monashensis* MSK03.

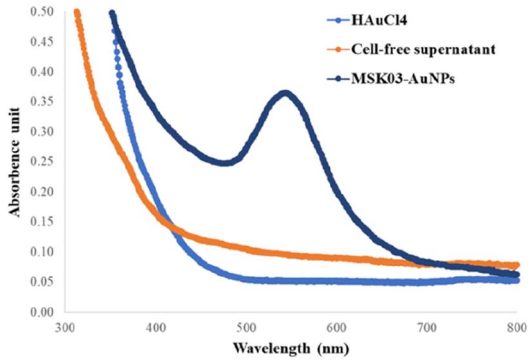

Fig. 3 UV-Vis spectra of MSK-AuNPs after incubation at 37 °C, 200 rpm for 72 h.

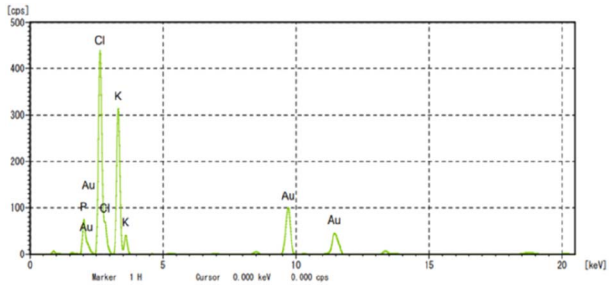

Fig. 4 Energy dispersive spectra of biosynthesized MSK03-AuNPs.

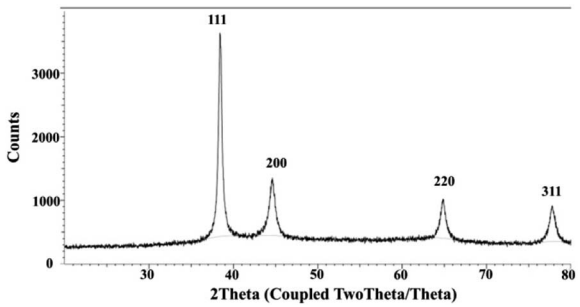

Fig. 5 The X-ray diffraction pattern of biosynthesized MSK03-AuNPs.

Additionally, XANES analysis was employed to investigate the local geometry and structure of gold in the synthesized AuNPs. Fig. 6 illustrates a comparison between the XANES spectra profiles of MSK03-AuNPs and a standard material. The spectra of MSK03-AuNPs exhibited a similar energy profile to that of Au metal foil, indicating a partial reduction of Au^{3+} to Au^0 during the biosynthesis process.

Based on the EDXRF, XRD, and XANES analyses, it can be concluded that *S. monashensis* MSK03 cell-free supernatants can effectively reduce Au^{3+} into Au^0. The detailed mechanism of the reduction process of Au^{3+} to Au^0 remains unclear. Several researchers have proposed the reducing agents for bio-synthesized AuNPs, including lipids, carbohydrates, nucleic acids, or proteins.[26] For the biosynthesized AuNPs using *Streptomyces* spp., cell wall reductive enzymes and enzymes on the

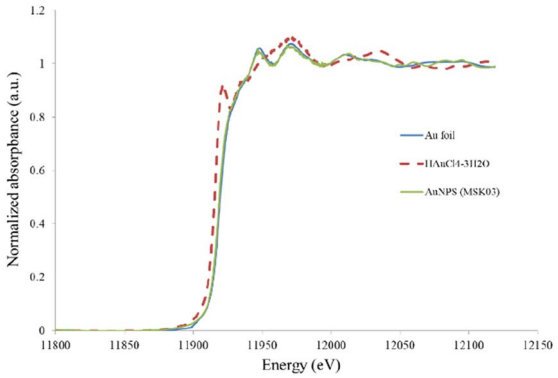

Fig. 6 XANES spectra of $HAuCl_4$, Au foil, and MSK03-AuNPs.

cytoplasmic membrane have been suggested as potential reducing agents.[28,55]

To identify the possible organic functional groups acting as capping, stabilizing, and reducing agents in the synthesized AuNPs, FTIR analysis was employed. The functional groups of biomolecules attached to the surface of AuNPs could play a role in the reduction of Au^{3+} to Au^0, making FTIR analysis crucial in identifying these biomolecules.[56,57] Fig. 7 presents the FTIR spectra of the cell-free supernatant of *S. monashensis* MSK03 and MSK03-AuNPs, each showing five major peaks. A shift in peak positions was observed from 3354, 1625, 1364, 1052, and 514 cm^{-1} in the cell-free supernatant of MSK03 to 3270, 1644, 1354, 1017, and 524 cm^{-1} in the MSK03-AuNPs, corresponding to N–H or O–H stretching, C=O stretching or N–H bending, C–N stretching or N–H bending, C–H stretching, and C–H

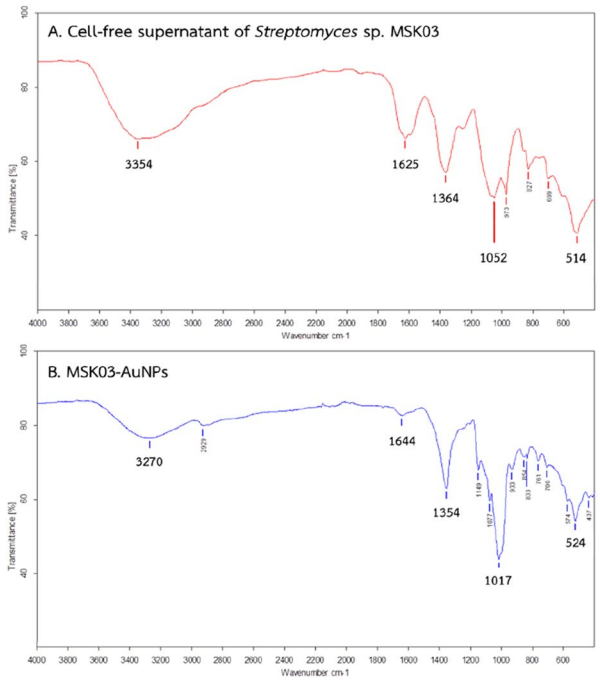

Fig. 7 FTIR spectra of (A) cell-free supernatant of *Streptomyces* sp. MSK03 and (B) MSK03-AuNPs.

bending or metal–ligand stretching, respectively. The absorption peaks at 3270, 1644, and 1354 cm^{-1} are indicative of functional groups associated with carbohydrates, amines, and amides, respectively, while the remaining peaks at 1017 and 524 cm^{-1} correspond to the amine functional groups of the protein. Changes in peak intensity or shifts in wavenumbers of functional groups from the cell-free supernatant to AuNPs can provide insights into the specific functional groups involved in the interaction with AuNPs.[58] For example, Kumar and Rao (2016) reported that proteins containing functional groups such as amide, carboxyl, and hydroxyl from *Streptomyces coelicoflavus* SRBVIT13 were attached to the surface of AuNPs, acting as stabilizing agents.[59] In our study, the FTIR results of the biosynthesized AuNPs using the extracellular cell-free supernatant of *S. monashensis* MSK03 indicated that proteins with functional groups like carboxyl, hydroxyl, amine, and amide groups from *S. monashensis* MSK03 are bound to AuNPs, serving as capping, reducing, and stabilizing agents.

TEM and DLS analyses were employed to evaluate the morphological properties (size and shape) of nanoparticles. The TEM technique typically focuses solely on the size of the core particle, excluding capping agents or other linked molecules.[60,61] The obtained images revealed that MSK03-AuNPs exhibited spherical forms (Fig. 8A). To confirm AuNPs formation and crystalline structure, SAED analysis revealed distinct diffraction rings, confirming the face-centered cubic (fcc) structure of gold (JCPDS: 04-0784), as indicated by (111), (200), (220), and (311) lattice planes (Fig. 8B).[30,62] The TEM/SAED results were consistent with the XRD results. The average particle size of MSK03-AuNPs was measured to be 23.2 ± 10.7 nm, with a size range varying from 7.1 to 40.0 nm (Fig. 8C). On the other hand, DLS measures the hydrodynamic size, which includes the core, capping agents, and other absorbed molecules on the nanoparticle's surface.[63,64] The analysis revealed that the MSK03-AuNPs exhibited an average size of 46.34 nm, with a polydispersity index (PDI) of 0.268 (Fig. 9). Previous reports have indicated that the particle size observed in TEM images is generally smaller than that measured by the DLS analyzer.[29,64–67] In our study, TEM analysis revealed the spherical shape of gold nanoparticles synthesized by MSK03, with an average particle size of 23.2 nm, which was smaller than the hydrodynamic size (46.34 nm) of the particles. The size of the nanomaterial is important because it affects its physical properties, cell penetration, and interactions with living cell molecules. Smaller particles have a larger surface area than larger particles for the same amount of material, and surface activity of AuNPs is also higher.[68]

Zeta potential analysis has been instrumental in understanding the stability of the synthesized nanostructures. This analytical technique is widely employed to describe the surface charge, stability, and aggregation conditions of colloidal particles, including AuNPs.[63,64,69] Large positive or negative zeta potential values indicate strong physical stability due to electrostatic repulsion among individual particles. Conversely, zeta potential values below −25 mV or above +25 mV typically indicate high stability.[70–75] Furthermore, studies have suggested that zeta potential values closer to −30 mV indicate higher stability for metal nanoparticles.[76,77] In our study, the zeta potential value of MSK03-AuNPs was determined to be −26.35 (±1.29) mV, indicating the presence of negative charge and potential repulsion among the AuNPs. This negative charge on the MSK03-AuNPs is attributed to the presence of biological molecules in the cell-free supernatant, which act as colloidal stabilizers for the MSK03-AuNPs. Consequently, our findings validate the high level of stability exhibited by MSK03-AuNPs.

Antimicrobial activity of MSK03-AuNPs

Due to the rise of microbial infections and increased drug-resistant rates, novel antimicrobials are being investigated. The World Health Organization (WHO) has prioritized pathogens under the acronym ESKAPE (*Enterococcus faecium*, *Staphylococcus aureus*, *K. pneumoniae*, *A. baumannii*, *P. aeruginosa*, and *Enterobacter* species) due to their profound threat to human health.[78] These antibiotic-resistant microorganisms can lead to severe and often fatal infectious diseases, such as bloodstream infections and pneumonia.[79] In this context, biosynthesized nanoparticles (NPs) have emerged as promising agents for addressing antibiotic-resistant infections, offering potential alternatives to conventional antibiotics.[80]

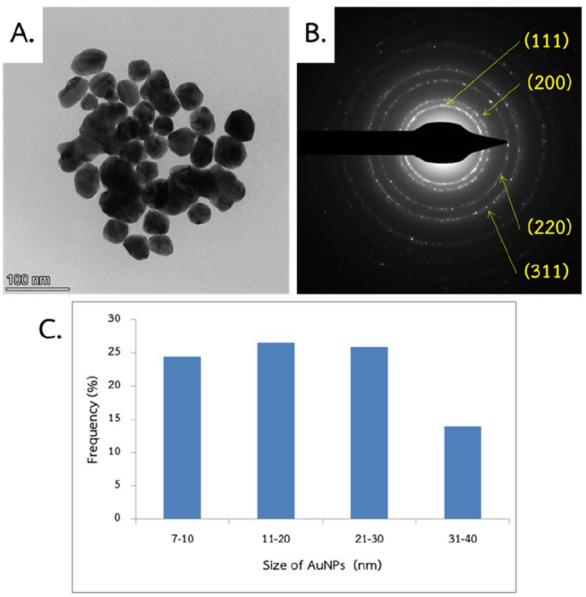

Fig. 8 TEM micrograph (A) and SAED pattern (B) and Particle size distribution (C) of MSK03-AuNPs.

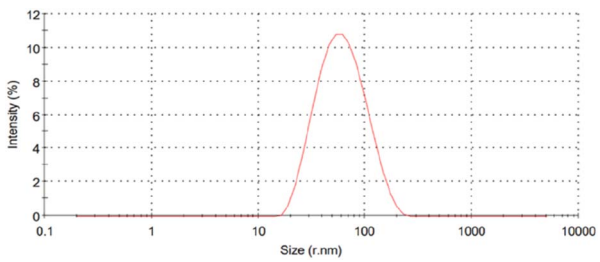

Fig. 9 The particle size distribution of biosynthesized MSK03-AuNPs.

Despite these advancements, there remains a dearth of studies on antibacterial gold nanoparticles (AuNPs) synthesized from actinomycetes.[27] This study addresses this gap by evaluating the antibacterial activity of MSK03-AuNPs against drug-resistant Gram-negative bacteria, specifically *P. aeruginosa* and *A. baumannii*, both recognized by the WHO as significant global threats. Multidrug-resistant strains of these bacteria present formidable challenges in treatment due to their extensive antimicrobial resistance, potential for outbreaks, and association with adverse outcomes such as increased mortality rates and treatment failure.[81–85] A systematic review identified that *A. baumannii* and *P. aeruginosa* infections had mortality rates of 47% and 23%, respectively.[83,85]

The antibacterial activity of MSK03-AuNPs, with an average particle size of 23.2 (±10.7) nm, was assessed using the agar well diffusion method. The inhibition zones for *P. aeruginosa* and *A. baumannii* were measured at 11.20 (±0.67) and 9.44 (±0.80) mm, respectively. Importantly, control substances, including $HAuCl_4$ and cell-free supernatant, exhibited no inhibitory effect (Table 1). Similarly, El-Batal and Tamie (2015) observed the sensitivity of the pathogen *P. aeruginosa* to AuNPs synthesized from the marine bacterium *Streptomyces cyaneus* Alex-SK121.[16] The AuNPs synthesized by strain Alex-SK121, with an average particle size of 12.63 nm, exhibited an inhibition zone of 26 ± 2 mm against *P. aeruginosa* when tested using the agar well diffusion method. Based on the information above, it has been demonstrated that smaller nanoparticles exhibit higher activity against pathogens compared to larger ones.

The mechanisms underlying the antimicrobial activity of AuNPs have been reported.[86] These nanoparticles operate in two stages: firstly, they alter the membrane potential and decrease adenosine triphosphate (ATP) synthase activity, thereby slowing down the metabolic process; secondly, they inhibit the ribosome's subunit for tRNA binding, effectively disrupting its biological process.[86,87] Remarkably, these actions are achieved while demonstrating lower toxicity to mammalian cells. In addition, the certain mechanisms of antimicrobial activity are required for further research.[86]

The antimicrobial activity of AuNPs synthesized by *Streptomyces* spp. against several Gram-positive and Gram-negative bacteria has been reported.[16–22] However, there has no report of antibacterial activity of AuNPs on *A. baumannii* (Table 1). Hence, our study marks the first investigation of the inhibitory effects of AuNPs, synthesized by *Streptomyces*, on the growth of *A. baumannii.* The findings from this study might be led the way for the development of new strategies to solving the problems caused by infections that are resistant to antibiotics. Future studies could explore the mechanistic details of MSK03-AuNPs' antimicrobial action, assess their possible clinical utility.

Cytotoxicity of MSK03-AuNPs

Cytotoxicity testing is a crucial approach to determining the safety of nanomaterials for potential biomedical use. Gold nanoparticles are commonly favored for biomedical applications due to their remarkable compatibility with human cells.[38] In this study, we evaluated the cytotoxicity of MSK03-AuNPs on Vero cell line using the MTT assay. MSK03-AuNPs at different concentration ranging from 32 to 512 μg mL^{-1} were tested for cytotoxicity. The IC_{50} of MSK03-AuNPs was greater than 512 μg mL^{-1}, indicating that the nanoparticles exhibited non-cytotoxicity on the Vero cell line. The viability of the Vero cell was greater than 92.5% after 24 hours of exposure to MSK03-AuNPs at a concentration of 512 μg mL^{-1}. It has been demonstrated that when cell viability remains above 80% following exposure to a test substance, the substance is considered non-toxic.[88,89] AuNPs synthesized from various natural sources, including plants and fungi, were evaluated for cytotoxicity using Vero cells, revealing no toxicity.[90–94] However, to the best of our knowledge, there have been no previous reports on the cytotoxicity of AuNPs synthesized by *Streptomyces* in Vero cells. Therefore, our study represents the first report of the cytotoxic effects of *Streptomyces*-synthesized AuNPs on Vero cells.

Our findings hold significance, as they indicate that AuNPs synthesized by *S. monashensis* MSK03 have the potential to act as effective antimicrobial agents against drug-resistant pathogens. The potential of AuNPs to interact with bacterial cells makes it feasible to conjugate antibiotics onto them. Thus, the AuNPs not only facilitate antibiotic penetration into bacteria but also have a synergistic effect.[95] Green synthesis AuNPs have been reported to have a synergistic effect with antibiotics. For instance, *Garcinia mangostana* extract was employed in one study to bio-synthesize AuNPs, which were then conjugated with streptomycin and azithromycin. The conjugated AuNPs had higher bactericidal efficiency against *Staphylococcus* spp. compared to free streptomycin and azithromycin.[96] Therefore, this synergistic effect could be used as an alternative to treat multidrug-resistant bacterial infections. Overall, the biocompatibility of AuNPs with human cells, as demonstrated by their

Table 1 Antimicrobial activity of MSK03-AuNPs and AuNPs synthesized by *Streptomyces* spp.[a]

	Inhibition zone (mm)						
		S. monashensis MSK03					
Tested pathogens	$HAuCl_4$	Supernatant	AuNPs	*Streptomyces cyaneus* Alex-SK121 (ref. 16)	*Streptomyces* sp. NH21 (ref. 17)	*Streptomyces griseus* M8 (ref. 19)	*Streptomyces* sp. U30 (ref. 21)
P. aeruginosa	0	0	11.20 ± 0.67	26 ± 2	0	20	23
A. baumanii	0	0	9.44 ± 0.80	ND	ND	ND	ND

[a] Each value represents the mean ± SD of three independent experiments; ND = not detect.

lack of cytotoxicity, makes them promising candidates for various biomedical applications. This is especially significant in the context of therapeutic medical treatments and drug delivery systems.

Conclusions

The findings of this study underscore the potential of actinomycetes as a valuable biological source for synthesizing gold nanoparticles. Our results demonstrate that a mixture of the cell-free supernatant from the actinomycetes strain *S. monashensis* MSK03 and 1 mM $HAuCl_4$ is favorable for the formation of AuNPs. The AuNPs, biosynthesized through the mediation of actinobacteria, were characterized using standard procedures, including UV-vis spectroscopy, XRD patterns, and XANES spectra, confirming the successful synthesis of AuNPs. FTIR results revealed that biological molecules, such as carboxyl, hydroxyl, amine, and amide groups, contributed to the reduction and stabilization of MSK03-AuNPs. The synthesized nanoparticles were spherical, with an average particle size of 23.2 nm and a surface charge of −26.35 mV. Gold nanoparticles derived from *S. monashensis* MSK03 exhibited activity against drug-resistant pathogens (*A. baumannii* and *P. aeruginosa*) while being non-toxic to the Vero cell line. Consequently, this study not only introduces a novel avenue for the biosynthesis of AuNPs but also highlights the significant potential of MSK03-derived gold nanoparticles as effective agents for future medical therapies.

Author contributions

SK: methodology, investigation, formal analysis, data curation, visualization, writing – original draft; PC: methodology, data curation, visualization, writing – review & editing; AR: methodology, data curation, visualization, writing – review & editing; WL: resources, formal analysis (FTIR, XRD, XANES), data curation, writing – review & editing; WP: data curation, writing – review & editing; PG: data curation, writing – review & editing; WS: data curation, writing – review & editing; MY: methodology, data curation, writing – review & editing; NN: conceptualization, methodology, project administration, supervision, validation, funding acquisition, writing – review & editing.

Conflicts of interest

There are no conflicts to declare.

Acknowledgements

This work was supported by Suranaree University of Technology, Thailand Science Research and Innovation (TSRI), and the National Science, Research, and Innovation Fund (NSRF) (FRB660044/0240 project code 180874) as well as the Center of Excellence on Environmental Health and Toxicology (EHT), OPS, Ministry of Higher Education, Science, Research and Innovation. Supavadee Kerdtoob extends gratitude to the External Grants and Scholarships for Graduate Students (One Research One Graduate: OROG), Suranaree University of Technology for providing tuition funding. We are deeply grateful to Assoc. Prof. Dr Nuannoi Chudapongse for her invaluable suggestions and contribution of $HAuCl_4$, which greatly enhanced the quality of this work.

References

1 M. Bhagat, S. Rajput, S. Arya, S. Khan and P. Lehana, *Bull. Mater. Sci.*, 2015, **38**, 1253–1258.
2 S. Shamaila, N. Zafar, S. Riaz, R. Sharif, J. Nazir and S. Naseem, *Nanomaterials*, 2016, **6**, 71.
3 S. Sathiyaraj, G. Suriyakala, A. Dhanesh Gandhi, R. Babujanarthanam, K. S. Almaary, T.-W. Chen and K. Kaviyarasu, *J. Infect. Public Health*, 2021, **14**, 1842–1847.
4 K. A. Altammar, *Front. Microbiol.*, 2023, **14**, 1155622.
5 X. Li, S. M. Robinson, A. Gupta, K. Saha, Z. Jiang, D. F. Moyano, A. Sahar, M. A. Riley and V. M. Rotello, *ACS Nano*, 2014, **8**, 10682–10686.
6 A. Sharma, S. Arya, D. Chauhan, P. R. Solanki, S. Khajuria and A. Khosla, *J. Mater. Res. Technol.*, 2020, **9**, 14321–14337.
7 B. Padha, S. Verma, Prerna, A. Ahmed, S. P. Patole and S. Arya, *Appl. Energy*, 2024, **356**, 122402.
8 S. B. Rana, R. P. P. Singh and S. Arya, *J. Mater. Sci.: Mater. Electron.*, 2017, **28**, 2660–2672.
9 K. R. B. Singh, P. Singh, S. Mallick, J. Singh and S. S. Pandey, *Int. J. Biol. Macromol.*, 2023, **253**, 127587.
10 P. Boomi, R. Ganesan, G. Prabu Poorani, S. Jegatheeswaran, C. Balakumar, H. Gurumallesh Prabu, K. Anand, N. Marimuthu Prabhu, J. Jeyakanthan and M. Saravanan, *Int. J. Nanomed.*, 2020, 7553–7568.
11 V. Nayak, K. R. B. Singh, R. Verma, M. D. Pandey, J. Singh and R. Pratap Singh, *Mater. Lett.*, 2022, **313**, 131769.
12 F. Khadivi Derakhshan, A. Dehnad and M. Salouti, *Synth. React. Inorg., Met.-Org., Nano-Met. Chem.*, 2012, **42**, 868–871.
13 M. Bhagat, R. Anand, R. Datt, V. Gupta and S. Arya, *J. Inorg. Organomet. Polym. Mater.*, 2019, **29**, 1039–1047.
14 K. S. Kumar, G. Kumar, E. Prokhorov, G. Luna-Bárcenas, G. Buitron, V. Khanna and I. Sanchez, *Colloids Surf. A Physicochem. Eng. Asp.*, 2014, **462**, 264–270.
15 P. Manivasagan, J. Venkatesan, K. Sivakumar and S.-K. Kim, *Microbiol. Res.*, 2014, **169**, 262–278.
16 A. El-Batal and M. Al Tamie, *J. Chem. Pharm. Res.*, 2015, **7**, 1020–1036.
17 M. Składanowski, M. Wypij, D. Laskowski, P. Golińska, H. Dahm and M. Rai, *J. Cluster Sci.*, 2017, **28**, 59–79.
18 S. Sadhasivam, P. Shanmugam, M. Veerapandian, R. Subbiah and K. Yun, *BioMetals*, 2012, **25**, 351–360.
19 M. M Hamed and L. S. Abdelftah, *Egypt. J. Aquat. Biol. Fish.*, 2019, **23**, 173–184.
20 B. Abirami, V. Akshata, M. Radhakrishnan, R. Namitha, K. Govindaraju, V. Gopikrishnan and K. Manigundan, *Int. J. Agric. Technol.*, 2023, **19**, 323–338.
21 R. Sayed and H. Saad, *Egypt. J. Chem.*, 2021, **64**, 7213–7222.
22 R. Balagurunathan, M. Radhakrishnan, R. B. Rajendran and D. Velmurugan, *Indian J. Biochem. Biophys.*, 2011, **48**, 331–335.

23 T. H. Al-Samarrai and J. Schmid, *Lett. Appl. Microbiol.*, 2000, **30**, 53–56.
24 D. Lane, 16S/23S rRNA Sequencing, in *Nucleic Acid Techniques in Bacterial Systematic*, ed. Stackebrandt E. and Goodfellow M., John Wiley and Sons, New York, 1991, pp. 115–175.
25 N. M. Soltani, B. G. Shahidi and N. Khaleghi, *Nanomedicine*, 2015, **2**, 153–159.
26 M. Shah, V. Badwaik, Y. Kherde, H. K. Waghwani, T. Modi, Z. P. Aguilar, H. Rodgers, W. Hamilton, T. Marutharaj and C. Webb, *Front. Biosci.*, 2014, **19**, 1320–1344.
27 M. Skladanowski, M. Wypij, D. Laskowski, P. Golinska, H. Dahm and M. Rai, *J. Cluster Sci.*, 2017, **28**, 59–79.
28 P. Manivasagan, J. Venkatesan, K. Sivakumar and S. K. Kim, *Crit. Rev. Microbiol.*, 2016, **42**, 209–221.
29 V. R. Ranjitha and V. R. Rai, *3 Biotech*, 2017, **7**, 299.
30 N. E.-A. El-Naggar, N. H. Rabei, M. F. Elmansy, O. T. Elmessiry, M. K. El-Sherbeny, M. E. El-Saidy, M. T. Sarhan and M. G. Helal, *Sci. Rep.*, 2023, **13**, 12686.
31 S. Shaikh, J. Fatima, S. Shakil, S. M. Rizvi and M. A. Kamal, *Saudi J. Biol. Sci.*, 2015, **22**, 90–101.
32 S. R. Sathish Kumar and K. V. Bhaskara Rao, *IET Nanobiotechnol.*, 2016, **10**, 308–314.
33 J. W. Jeffery, *Methods in X-ray Crystallography*, Academic Press, London, 1971.
34 G. S. Henderson, F. M. De Groot and B. J. Moulton, *Rev. Mineral. Geochem.*, 2014, **78**, 75–138.
35 Y. Konishi, T. Tsukiyama, N. Saitoh, T. Nomura, S. Nagamine, Y. Takahashi and T. Uruga, *J. Biosci. Bioeng.*, 2007, **103**, 568–571.
36 S. Vijayakumar and S. Ganesan, *J. Nanomater.*, 2012, **2012**, 14.
37 V. Pivodová, J. Franková, A. Galandáková and J. Ulrichová, *Nanobiomedicine*, 2015, **2**, 7.
38 P. C. Chen, S. C. Mwakwari and A. K. Oyelere, *Nanotechnol. Sci. Appl.*, 2008, 45–65.
39 M. Drancourt, P. Berger and D. Raoult, *J. Clin. Microbiol.*, 2004, **42**, 2197–2202.
40 N. Pantidos and L. E. Horsfall, *J. Nanomed. Nanotechnol.*, 2014, **5**, 1.
41 S. B. Zotchev, *J. Biotechnol.*, 2012, **158**, 168–175.
42 L. Wang, C. Hu and L. Shao, *Int. J. Nanomed.*, 2017, **12**, 1227–1249.
43 X. Hu, Y. Zhang, T. Ding, J. Liu and H. Zhao, *Front. Bioeng. Biotechnol.*, 2020, **8**, 990.
44 M. Shah, V. D. Badwaik and R. Dakshinamurthy, *J. Nanosci. Nanotechnol.*, 2014, **14**, 344–362.
45 Y. N. Slavin, J. Asnis, U. O. Häfeli and H. Bach, *J. Nanobiotechnol.*, 2017, **15**, 1–20.
46 M. Hassanisaadi, G. H. S. Bonjar, A. Rahdar, S. Pandey, A. Hosseinipour and R. Abdolshahi, *Nanomaterials*, 2021, **11**, 2033.
47 T. Bennur, Z. Khan, R. Kshirsagar, V. Javdekar and S. Zinjarde, *Sensor. Actuator. B Chem.*, 2016, **233**, 684–690.
48 D. Prakash, V. Mahale, A. Bankar, N. Nawani, V. Mahale and D. Prakash, *Indian J. Exp. Biol.*, 2013, **51**, 969–972.
49 N. F. Zonooz, M. Salouti, R. Shapouri and J. Nasseryan, *J. Cluster Sci.*, 2012, **23**, 375–382.
50 M. Sapkal and A. Deshmukh, *Res. J. Biotechnol.*, 2008, **3**, 36–39.
51 A. Sharma, S. Sharma, K. Sharma, S. P. Chetri, A. Vashishtha, P. Singh, R. Kumar, B. Rathi and V. Agrawal, *J. Appl. Phycol.*, 2016, **28**, 1759–1774.
52 G. E. J. Poinern, *A Laboratory Course in Nanoscience and Nanotechnology*, CRC Press, 2014.
53 H.-S. Kim, Y. Seo, K. Kim, J. W. Han, Y. Park and S. Cho, *Nanoscale Res. Lett.*, 2016, **11**, 230.
54 K. Ricketts, C. Guazzoni, A. Castoldi and G. Royle, *Nucl. Instrum. Methods Phys. Res. Sect. A Accel. Spectrom. Detect. Assoc. Equip.*, 2016, **816**, 25–32.
55 A. Ahmad, S. Senapati, M. I. Khan, R. Kumar, R. Ramani, V. Srinivas and M. Sastry, *Nanotechnology*, 2003, **14**, 824.
56 T. Elavazhagan and K. D. Arunachalam, *Int. J. Nanomed.*, 2011, **6**, 1265.
57 S. A. Dahoumane, E. K. Wujcik and C. Jeffryes, *Enzyme Microb. Technol.*, 2016, **95**, 13–27.
58 W. K. A. Wan Mat Khalir, K. Shameli, S. D. Jazayeri, N. A. Othman, N. W. Che Jusoh and N. M. Hassan, *Front. Chem.*, 2020, **8**, 620.
59 S. R. Sathish Kumar and K. V. Bhaskara Rao, *IET Nanobiotechnol.*, 2016, **10**, 308–314.
60 B. Schaffer, U. Hohenester, A. Trügler and F. Hofer, *Phys. Rev. B: Condens. Matter Mater. Phys.*, 2009, **79**, 041401.
61 M. Montes, A. Mayoral, F. Deepak, J. Parsons, M. Jose-Yacamán, J. Peralta-Videa and J. Gardea-Torresdey, *J. Nanopart. Res.*, 2011, **13**, 3113–3121.
62 S. Akhtar, S. M. Asiri, F. A. Khan, S. T. Gunday, A. Iqbal, N. Alrushaid, O. A. Labib, G. R. Deen and F. Z. Henari, *Arab. J. Chem.*, 2022, **15**, 103594.
63 a. k. Mittal, A. Kaler, A. Mulay and U. Banerjee, *J. Nanoparticles*, 2013, 2013.
64 A. Muthuvel, K. Adavallan, K. Balamurugan and d. n. k. Narendran, *Biomed. Prev. Nutr.*, 2014, **4**, 325–332.
65 C. H. N. de Barros, G. C. F. Cruz, W. Mayrink and L. Tasic, *Nanotechnol. Sci. Appl.*, 2018, 1–14.
66 R. I. MacCuspie, K. Rogers, M. Patra, Z. Suo, A. J. Allen, M. N. Martin and V. A. Hackley, *J. Environ. Monit.*, 2011, **13**, 1212–1226.
67 T. G. Souza, V. S. Ciminelli and N. D. S. Mohallem, *J. Phys.: Conf. Ser.*, 2016, **773**, 012039.
68 C. Liang, J. Y. Cheong, G. Sitaru, S. Rosenfeldt, A. S. Schenk, S. Gekle, I.-D. Kim and A. Greiner, *Adv. Mater. Interfaces*, 2022, **9**, 2100867.
69 F. Graily-Moradi, A. Maadani Mallak and M. Ghorbanpour, in *Biogenic Nano-Particles and Their Use in Agro-Ecosystems*, Springer, 2020, pp. 187–204.
70 S. L. Brock, *Nanostructures and Nanomaterials*, Imperial College Press, London, 2004.
71 J. D. Clogston and A. K. Patri, *Methods Mol. Biol.*, 2011, **697**, 63–70.
72 J. D. Clogston and A. K. Patri, in *Characterization of Nanoparticles Intended for Drug Delivery*, Springer, 2011, pp. 63–70.

73 M. Horie and K. Fujita, in *Advances in molecular toxicology*, Elsevier, 2011, vol. 5, pp. 145–178.
74 K. E. Sapsford, K. M. Tyner, B. J. Dair, J. R. Deschamps and I. L. Medintz, *Anal. Chem.*, 2011, **83**, 4453–4488.
75 A. J. Shnoudeh, I. Hamad, R. W. Abdo, L. Qadumii, A. Y. Jaber, H. S. Surchi and S. Z. Alkelany, in *Biomaterials and Bionanotechnology*, ed. R. K. Tekade, Academic Press, 2019, pp. 527–612.
76 A. Gade, A. Ingle, C. Whiteley and M. Rai, *Biotechnol. Lett.*, 2010, **32**, 593–600.
77 M. Rai, A. Ingle, S. Gaikwad, I. Gupta, A. Gade and S. Silvério da Silva, *J. Appl. Microbiol.*, 2016, **120**, 527–542.
78 G. Mancuso, A. Midiri, E. Gerace and C. Biondo, *Pathogens*, 2021, **10**, 1310.
79 Z. Breijyeh, B. Jubeh and R. Karaman, *Molecules*, 2020, **25**, 1340.
80 N. Gürsoy, B. Y. Öztürk and İ. Dağ, *Turk. J. Biol.*, 2021, **45**, 196–213.
81 H. Giamarellou and I. Karaiskos, *Antibiotics*, 2022, **11**, 1009.
82 D. Alrahmany, A. Omar, A. Alreesi, G. Harb and I. Ghazi, *Antibiotics*, 2022, **11**, 1086.
83 A. Vivo, M. A. Fitzpatrick, K. J. Suda, M. M. Jones, E. N. Perencevich, M. A. Rubin, S. Ramanathan, G. M. Wilson, M. E. Evans and C. T. Evans, *BMC Infect. Dis.*, 2022, **22**, 491.
84 C. J. Kim, K. H. Song, N. K. Choi, J. Ahn, J. Y. Bae, H. J. Choi, Y. Jung, S. S. Lee, J. H. Bang, E. S. Kim, S. M. Moon, J. E. Song, Y. G. Kwak, S. H. Chun, Y. S. Kim, K. H. Park, Y. M. Kang, P. G. Choe, S. Lee and H. B. Kim, *Sci. Rep.*, 2022, **12**, 13934.
85 D. Alrahmany, A. F. Omar, A. Alreesi, G. Harb and I. M. Ghazi, *Antibiotics*, 2022, **11**, 1086.
86 Y. Cui, Y. Zhao, Y. Tian, W. Zhang, X. Lu and X. Jiang, *Biomaterials*, 2012, **33**, 2327–2333.
87 T. Al Hagbani, S. M. D. Rizvi, T. Hussain, K. Mehmood, Z. Rafi, A. Moin, A. S. Abu Lila, F. Alshammari, E.-S. Khafagy, M. Rahamathulla and M. H. Abdallah, *Polymers*, 2022, **14**, 771.
88 R. Chen, K. Qiu, G. Han, B. K. Kundu, G. Ding, Y. Sun and J. Diao, *Chem. Sci.*, 2023, **14**, 10236.
89 J. López-García, M. Lehocký, P. Humpolíček and P. Sáha, *J. Funct. Biomater.*, 2014, **5**, 43–57.
90 P. Priya Tharishini, N. Saraswathy, K. Smila, D. Yuvaraj, M. Chandran and P. Vivek, *Int. J. ChemTech Res.*, 2014, **6**, 4241–4250.
91 M. A. Meléndez-Villanueva, K. Morán-Santibañez, J. J. Martínez-Sanmiguel, R. Rangel-López, M. A. Garza-Navarro, C. Rodríguez-Padilla, D. G. Zarate-Triviño and L. M. Trejo-Ávila, *Viruses*, 2019, **11**, 1111.
92 K. Priya and P. R. Iyer, *Egypt. Liver J.*, 2020, **10**, 15.
93 M. K. Soliman, S. S. Salem, M. Abu-Elghait and M. S. Azab, *Appl. Biochem. Biotechnol.*, 2023, **195**, 1158–1183.
94 V. Nachiyar, S. Sunkar and P. Prakash, *Der Pharma Chem.*, 2015, **7**, 31–38.
95 S. M. D. Rizvi, A. S. A. Lila, A. Moin, T. Hussain, M. A. Kamal, H. Sonbol and E.-S. Khafagy, *Pharmaceutics*, 2023, **15**, 430.
96 R. Nishanthi, P. Palani, *16th International Conference of Nanotechnology*, Japan, 2016.